Temperature dependence of thermal expansion and elastic constants of single crystals of ZrB2 and the suitability of ZrB2 as a substrate for GaN film

AUTHOR(S):

Okamoto, NL; Kusakari, M; Tanaka, K; Inui, H; Yamaguchi, M; Otani, S

CITATION:

Okamoto, NL ...[et al]. Temperature dependence of thermal expansion and elastic constants of single crystals of ZrB2 and the suitability of ZrB2 as a substrate for GaN film. JOURNAL OF APPLIED PHYSICS 2003, 93(1): 88-93

ISSUE DATE:

2003-01-01

URL:

http://hdl.handle.net/2433/50066

Temperature dependence of thermal expansion and elastic constants of single crystals of ZrB_2 and the suitability of ZrB_2 as a substrate for GaN film

Norihiko L. Okamoto, Misato Kusakari, Katsushi Tanaka, Haruyuki Inui, and Masaharu Yamaguchi
Department of Materials Science and Engineering, Kyoto University, Sakyo-ku, Kyoto 606-8501, Japan

Shigeki Otani
Advanced Materials Laboratory, National Institute for Materials Science 1-1, Namiki, Tsukuba, Ibaraki 305-0044, Japan

(Received 19 July 2002; accepted 8 October 2002)

Coefficients of thermal expansion (CTE) and elastic constants of single crystals of ZrB_2 have been determined in the temperature ranges from room temperature to 1073 K and from room temperature to 1373 K, respectively. The elastic constants of ZrB_2 are best characterized by the large value of the Young modulus (as high as 500 GPa) and the small values of the Poisson ratio (0.13–0.15), indicating the high stiffness and hardness and the brittleness, respectively. The values of CTE along the *a*- and *c*-axis directions are 6.66×10^{-6} and 6.93×10^{-6} K^{-1}, respectively, when averaged over the temperature range from room temperature to 1073 K. The CTE value along the *a*-axis direction of ZrB_2 is only moderately larger than the corresponding value for GaN. This together with the small lattice mismatch along the *a*-axis direction between ZrB_2 and GaN in the heteroepitaxial orientation relationship of $(0001)_{GaN}//(0001)_{ZrB_2}$ and $\langle 11\bar{2}0\rangle_{GaN}//\langle 11\bar{2}0\rangle_{ZrB_2}$ indicate that only a small compressive stress develops in the GaN thin-film crystal grown on the (0001) surface of the ZrB_2 substrate. The stresses developed in the GaN thin-film crystal are evaluated with the values of CTE and elastic constants of ZrB_2 determined in the present study. The evaluation verifies the suitability of ZrB_2 as a substrate for heteroepitaxial growth of GaN. © *2003 American Institute of Physics.* [DOI: 10.1063/1.1525404]

I. INTRODUCTION

Many transition-metal diborides with the hexagonal AlB_2 structure (space group: $P6/mmm$) exhibit attractive properties such as high melting temperature, high stiffness and hardness and high electrical and thermal conductivity.[1–3] ZrB_2 is one of these diborides and is in practical use as refractory crucibles and sheaths in steel making industries because of its high corrosion-resistance in addition to these attractive properties.[1–3] In recent years, ZrB_2 is being considered for the use in the thermal protection system of hypersonic vehicles in the form of composites reinforced with SiC and C because of the excellent heat and thermal shock resistance.[4] On top of that, ZrB_2 is also recently considered for the use as a substrate for heteroepitaxial growth of GaN in the form of single crystal because of the small lattice mismatch.[5–7] The quality of the grown GaN crystal is recently reported to be much higher on the ZrB_2 substrate than on α(6H)–SiC (Refs. 7, 8) and sapphire[9–11] substrates, which have been usually used to date.

Single crystals of ZrB_2 may exhibit highly anisotropic physical properties when its crystal structure is considered. Its hexagonal structure is basically a layered structure in which pure Zr and pure B atomic planes stack alternatively along the *c*-axis. However, only a little is known about physical properties of single crystals such as thermal expansion, elastic constants, electrical and thermal conductivity, although these data are available for the polycrystals.[1–3,12] This may stem from the fact that the very high melting temperature (3060 °C) makes single-crystal growth difficult. However, one of the authors has recently succeeded in growing large-size single crystals of ZrB_2 by the rf heated floating-zone method.[13,14]

In the present study, we investigate thermal expansion and elastic constants of single crystals of ZrB_2 as a function of crystal orientation and temperature for the first time and discuss anisotropic nature of the elastic and thermal properties. We then evaluate stresses developed in a GaN thin-film crystal grown on the (0001) ZrB_2 substrate for the case of heteroepitaxial growth with the orientation relationship of $(0001)_{GaN}//(0001)_{ZrB_2}$ and $\langle 11\bar{2}0\rangle_{GaN}//\langle 11\bar{2}0\rangle_{ZrB_2}$ and compare them with similarly evaluated stresses for the case of GaN growth on the (0001) surface of 6H–SiC and sapphire substrates in order to check the suitability of ZrB_2 as a substrate for heteroepitaxial growth of GaN.

II. EXPERIMENTAL PROCEDURES

Single crystals of ZrB_2 were grown by the rf heated floating-zone method as described previously.[13,14] After determining the crystallographic orientations by the x-ray back reflection Laue method, specimens with a rectangular parallelepiped shape having three orthogonal faces parallel to the (0001), $(11\bar{2}0)$, and $(1\bar{1}00)$ planes were cut from the crystal

TABLE I. Dimensions of specimens used for the measurements of elastic constants and coefficients of thermal expansion.

Dimensions (mm)		$[1\bar{1}00]$	$[11\bar{2}0]$	[0001]
CTE	*a*-axis	2.843	6.862	2.809
	c-axis	2.866	2.762	7.910
Elastic constant		3.694	3.673	3.762

by spark-machining. Then, the specimen surface was mechanically polished with diamond paste. The maximum error in parallelism for each face was at most 3 μm/mm. The deviation from the respective crystallographic orientation was smaller than 0.2° for each face. The dimensions of specimens used for the measurements of coefficients of thermal expansion (CTE) and elastic constants are summarized in Table I.

Measurements of the CTE were carried out with a push-rod type differential dilatometer (Shimazdu TMA50) in the temperature range from room temperature to 1073 K at the heating rate of 5 K per minute under Ar gas flow. Measurements of the elastic constants were carried out by the rectangular parallelepiped resonance (RPR) method in the temperature range from room temperature to 1373 K. In this method, all elastic constants are derived from the frequencies of the resonance vibrations of specimen.[15]

III. RESULTS

Thermal expansion of ZrB_2 measured along the *a*- and *c*-axis directions is plotted, respectively, in Figs. 1(a) and 1(b) as relative elongation with respect to the original specimen length at room temperature. Coefficients for thermal expansion (CTE) averaged over some temperature ranges are indicated in the figures. The value of CTE averaged over the temperature range from room temperature to 1073 K is only a little larger for along the *c*-axis (6.93×10^{-6} K^{-1}) than for along the *a*-axis (6.66×10^{-6} K^{-1}). The rather isotropic thermal expansion behavior is somewhat surprising when considering the hexagonal crystal structure of ZrB_2 in which pure Zr and pure B atomic planes stack alternatively along the *c*-axis. Although ZrB_2 exhibits a metallic nature of electrical conductivity, the values of the CTE for ZrB_2 are considerably smaller than those reported for usual metals and alloys and are comparable to those reported for many ceramics. While the *a*-axis CTE value for ZrB_2 is only moderately larger than that for GaN (5.59×10^{-6} K^{-1}), the *c*-axis CTE value for ZrB_2 is considerably larger than the corresponding value for GaN (3.17×10^{-6} K^{-1}).[16] The *a*-axis CTE value for ZrB_2 is smaller than the corresponding value for sapphire (7.5×10^{-6} K^{-1}).[17]

The single-crystal elastic constants of ZrB_2 are plotted in Fig. 2 as a function of temperature. Values of the c_{11}, c_{33}, and c_{44} elastic constants decrease monotonically with the increase in temperature, while the values of c_{12} and c_{13} are virtually temperature independent. Data points for each of the five elastic constants are fitted to a linear equation in the form of

$$c_{ij}=c_{ij\,(RT)}+k(T-300), \tag{1}$$

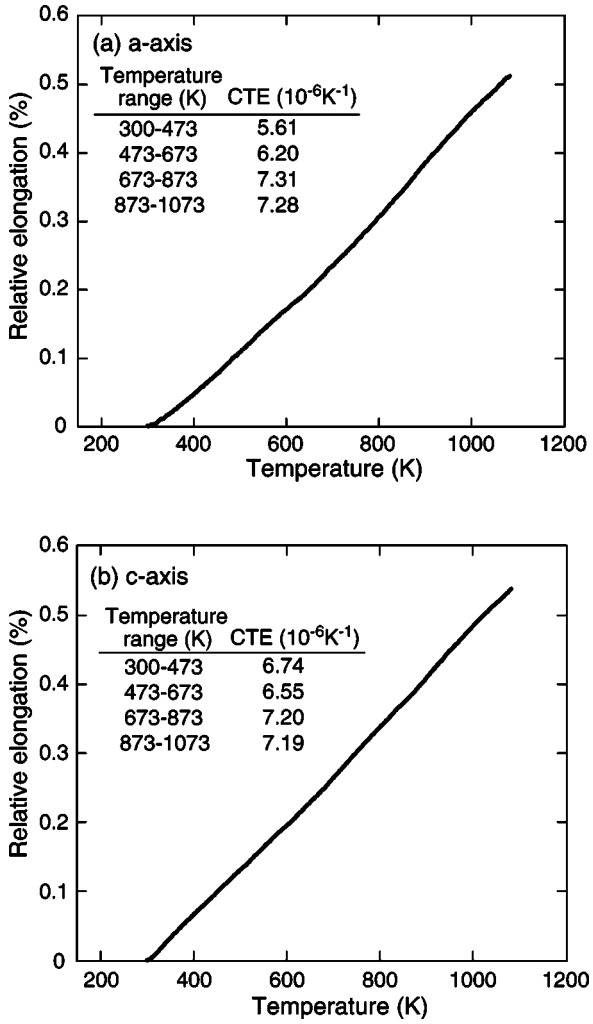

FIG. 1. Thermal expansion of ZrB_2 measured along (a) *a*- and (b) *c*-axis directions plotted as the relative elongation with respect to the original specimen length at room temperature. Coefficients for thermal expansion (CTE) averaged over some temperature ranges are indicated in the figure.

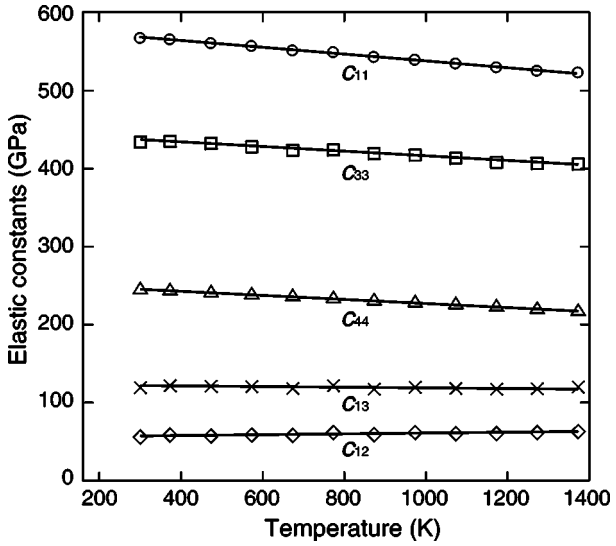

FIG. 2. Five independent single-crystal elastic constants of ZrB_2 plotted as a function of temperature.

TABLE II. Single-crystal elastic constants of ZrB_2 in the form of $c_{ij} = c_{ij(RT)} + k(T\text{-}300)$, where $c_{ij(RT)}$, k, and T stand, respectively, for the elastic constant at room temperature, numerical constant, and temperature in Kelvin.

c_{ij}	$c_{ij(RT)}$ (GPa)	k
c_{11}	567.8	−0.0431
c_{33}	436.1	−0.0294
c_{12}	56.9	0.0051
c_{13}	120.5	−0.0022
c_{44}	247.5	−0.0261

where $c_{ij\,(RT)}$, k, and T stand, respectively, for the elastic constant at room temperature, numerical constant, and temperature in Kelvin, as tabulated in Table II. Values of all the five independent elastic constants of ZrB_2 are larger than those for usual metal and alloys, being consistent with the high melting temperature. Of the five elastic constants, the values of c_{12} and c_{13} are notably small, indicating the brittleness of the boride. Anisotropic parameters (c_{13}/c_{12}, c_{44}/c_{66}, and c_{33}/c_{11}) are deduced from Fig. 2 and are plotted in Fig. 3 as a function of temperature. Both the large c_{13}/c_{12} and small c_{33}/c_{11} values indicate that atomic bonding along the *a*-axis is stronger than that along the *c*-axis, being consistent with the fact that the crystal structure of ZrB_2 is a layered-type with respect to the *c*-axis.

Polycrystalline elastic constants are evaluated from the single-crystal elastic constants by the Hill's method. The temperature dependence of the bulk, Young and shear moduli as well as that of the Poisson ratio is illustrated in Fig. 4(a). As in the case of single-crystal elastic constants, the bulk, Young's, and shear moduli monotonically decrease with increasing temperature. Values of these three moduli decrease, respectively, by 4.5%, 9.1%, and 10.4% when the temperature is increased from room temperature to 1373 K. The value of the Young modulus is as high as 500 GPa, being consistent with the high stiffness and hardness reported to date. On the other hand, the value of the Poisson ratio increases with increasing temperature from 0.133 at room temperature to 0.151 at 1373 K. However, these values of the Poisson ratio are very small, again indicating the brittleness of the boride. The orientation dependence of the Young modulus on prism plane at room temperature and 1373 K is depicted in Fig. 4(b). The curves in Fig. 4(b) are calculated with the following equation:

$$1/E = s_{11}\cdot\sin^4\theta + s_{33}\cdot\cos^4\theta + (s_{44}+2s_{13})\sin^2\theta\cdot\cos^2\theta, \quad (2)$$

where θ is the angle between the corresponding tensile (compressive) direction and the *c*-axis, and s_{ij} is elastic compliance constants. Since crystals with the hexagonal symmetry are elastically isotropic around the *c*-axis, the Young modulus does not vary with orientation on basal plane. As seen in Fig. 4(b), the tendency for the orientation dependence does not significantly vary with temperature. While the values of

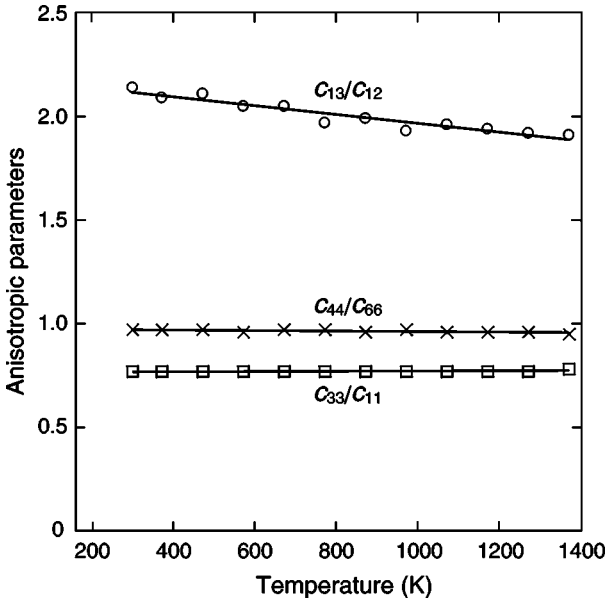

FIG. 3. Anisotropic parameters (c_{13}/c_{12}, c_{44}/c_{66}, and c_{33}/c_{11}) plotted as a function of temperature.

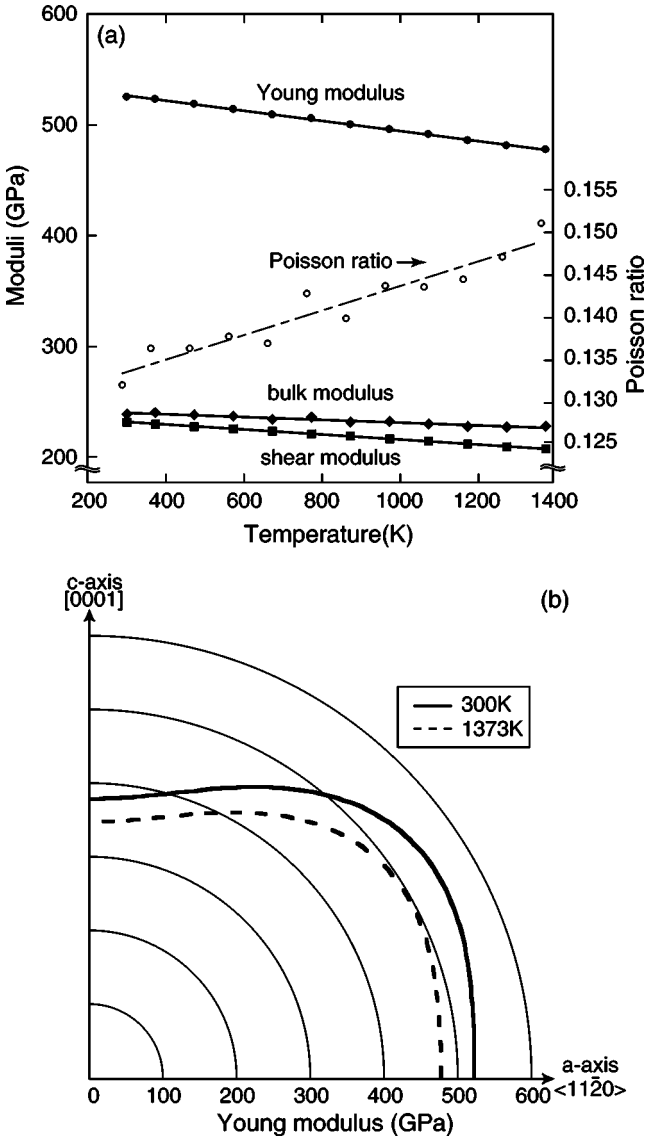

FIG. 4. (a) Temperature dependence of bulk, Young, shear moduli, and Poisson ratio of ZrB_2 and (b) orientation dependence of the Young modulus on the prism plane at room temperature and 1373 K.

the Young modulus exhibit a maximum at a direction approximately 30° from the *a*-axis, the value along the *a*-axis is larger than that along the *c*-axis. This again implies that atomic bonding is stronger along the *a*-axis than along the *c*-axis.

IV. DISCUSSION

ZrB_2 is being considered for the use as a substrate for heteroepitaxial growth of GaN in the form of a single crystal.[5,6] GaN with the hexagonal wurtzite structure is one of the most promising light-emitting devices in the region of blue to ultraviolet light with a band gap of 3.39 eV.[18] So far, heteroepitaxial growth of single crystalline GaN has been made with the use of the (0001) surface of sapphire or α(6H)−SiC single-crystal substrates. However, the quality of the GaN crystal grown on top of a sapphire substrate is not good and usually contains many dislocations because of the large lattice mismatches between the two materials.[19] When 6H−SiC is used as a substrate, on the other hand, while the lattice mismatch is better, many cracks are frequently observed in the grown GaN crystal because of the tensile stress developed in the grown GaN crystal during cooling from the formation temperature due to the smaller thermal expansion of 6H−SiC.[20] From this perspective, ZrB_2 seems to be an excellent substrate for heteroepitaxial growth of GaN when the growth is made on the (0001) surface with the orientation relationship of $(0001)_{GaN}//(0001)_{ZrB_2}$ and $\langle 11\bar{2}0\rangle_{GaN}//\langle 11\bar{2}0\rangle_{ZrB_2}$, since the *a*-axis lattice mismatch is small (0.63%) and only a small compressive stress is expected to develop in the grown GaN crystal due to a little larger thermal expansion of ZrB_2. In the following, we will quantitatively evaluate stresses that develop in the GaN crystal grown on a substrate during cooling from a high temperature, at which GaN films are formed from vapor, with the use of the values of thermal expansion coefficients and elastic constants determined in the present study. For simplicity, we use the average value of the CTE of ZrB_2 over the temperature range from room temperature to 1073 K (6.66×10^{-6} K^{-1} along the *a*-axis), independent of temperature in the calculation. For GaN, the values of elastic constants and CTE are referred to Refs. 21 and 16, respectively. The lattice constants of ZrB_2 and GaN at high temperatures $[a_{(T)}]$ are calculated by multiplying the values at room temperature (a_{RT}) by the CTE [i.e., $a_{(T)}=(1+\alpha\Delta T)a_{RT}$]. We also made similar calculations for the case of 6H−SiC and sapphire substrates for comparison, with the use of values of thermal expansion coefficients and elastic constants tabulated in Table III.

In order to quantitatively deduce stresses developed in the GaN thin-film crystal grown on a substrate, we calculate the interfacial stress that is caused by mismatches in the lattice constants (only the *a*-axis values are taken into account) and elastic constants. Since the interfacial area is far larger than the thickness of the GaN thin-film crystal, the calculated interfacial stress can be considered to be the stress developed in the thin film (the film stress). We take two different simple models for the calculation. In one model, we calculate the interfacial stress as a function of temperature on the basis

TABLE III. Parameters used in the calculation of interfacial stress between GaN and ZrB_2, 6H−SiC and sapphire substrates.

	GaN	ZrB_2	6H−SiC	Sapphire
A-axis lattice constant (Å)	3.189[a]	3.169[b]	3.081[c]	2.747[c] (4.758)
Lattice mismatch (%)	⋯	0.6	3.4	13.9
$\alpha_{a\text{-axis}}$ (10^{-6} K^{-1})	5.59[a]	6.66[f]	4.2[c]	7.5[c]
$E_{a\text{-axis(RT)}}$ (GPa)	309.6[d]	533.2[f]	447.1[d]	432.1[e]

[a]Reference 16.
[b]B. Post, *Boron, Metallo-Boron Compounds and Borones* (Wiley, New York, 1964).
[c]Reference 17.
[d]Reference 21.
[e]T. Goto *et al.*, J. Geophysical Res. **94** (B6), 7588 (1989).
[f]Present study.

that no misfit dislocations are introduced at the interface on the formation. In this case, a finite value of the interfacial stress is generated at the formation temperature and the interfacial stress changes with temperature on cooling down to room temperature. In this model, the stress generated at the interface is expressed by

$$\sigma_{film}=-E_{substrate}\cdot\varepsilon_{substrate}=E_{GaN}\cdot\varepsilon_{GaN}, \tag{3}$$

$$\varepsilon_{total}=\varepsilon_{GaN}-\varepsilon_{substrate}$$
$$=(a_{substrate}-a_{GaN})\Big/\left(\frac{a_{GaN}+a_{substrate}}{2}\right), \tag{4}$$

where σ, E, ε, and a stand, respectively, for interfacial stress, Young's modulus along the *a*-axis, misfit strain, and *a*-axis lattice constant. The calculation results are illustrated in Fig. 5(a) as a function of temperature. In this calculation, the interfacial stress generated at the interface (i.e., the stress developed in the GaN thin-film) is simply as a function of temperature regardless of the film-formation temperature, i.e., the film stress at room temperature (after cooling) does not depend on the film-formation temperature. As seen Fig. 5(a), the film stress is in compression for all three substrates, since the *a*-axis lattice parameters for these three substrates are all greater than that for GaN. The film stress generated in GaN increases with decreasing temperature for ZrB_2 and sapphire substrates, while it decreases with decreasing temperature for the SiC substrate. This results from the fact that the CTE values for the former two substrates is larger than that for GaN while the CTE value for the latter substrate is smaller than that for GaN. The film stress for the sapphire substrate is in compression and is huge, indicating the necessity for the introduction of misfit dislocations on the film formation. This is consistent with the experimental observation of many dislocations in GaN thin films grown on sapphire.[19] On the other hand, the film stress for the SiC substrate is much smaller than that for the sapphire substrate, because of the better lattice mismatch with GaN. But the film stress in this case is in compression, which is not consistent with the experimental observation that the tensile stress causes many cracks in GaN thin films grown on 6H−SiC.[20] This may indicate that misfit dislocations are introduced in the formation of GaN films on 6H−SiC so that the film stress

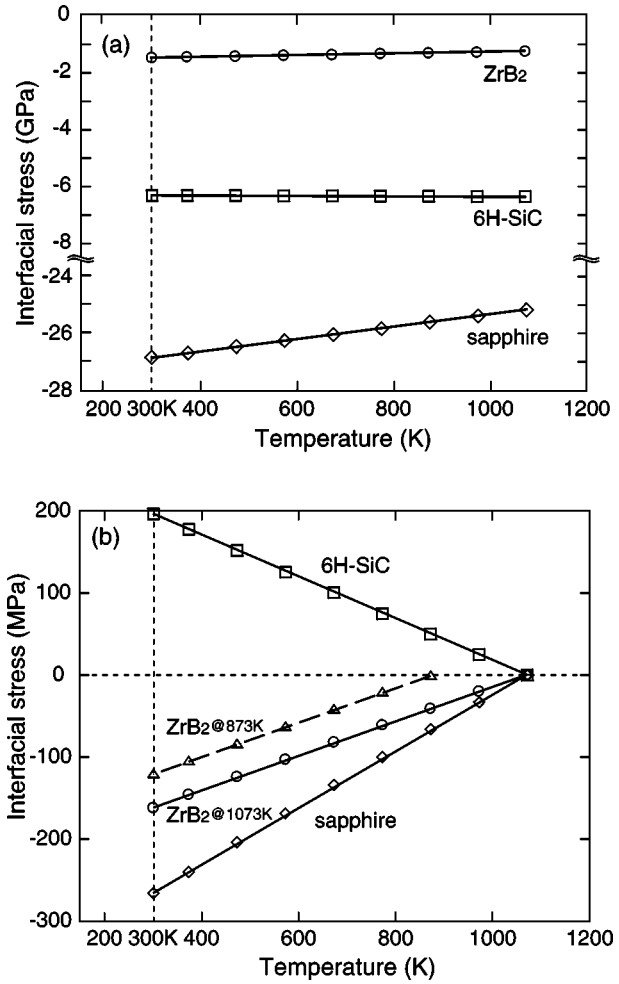

FIG. 5. The interfacial stress generated at the interface between GaN and ZrB_2, SiC and sapphire substrates calculated (a) with Eqs. (3) and (4) and (b) with Eqs. (3) and (5).

(in compression) is considerably reduced in the film formation, as will be shown later in Fig. 5(b). The film stress for the ZrB_2 substrate is also in compression and is much smaller than those for SiC and sapphire substrates. The film stress at room temperature for the ZrB_2 substrate is as small as 1.23 GPa, while those for SiC and sapphire substrates are 6.30 and 26.86 GPa, respectively. This small value of the film stress obviously comes from the fact that the lattice mismatch between GaN and ZrB_2 is very small and the value of the CTE for ZrB_2 are only a little larger than that for GaN.

In the second model, we calculate the interfacial stress as a function of temperature on the basis that no mismatch stress is generated at the interface at the film-formation temperature, assuming the mismatch is fully relaxed through the introduction of misfit dislocations, and that the mismatch stress is generated during cooling from the formation temperature due to changes in the mismatch. This can occur if the lattice mismatch on the formation of GaN thin films is large enough to introduce many misfit dislocations, as typically seen for the case of the sapphire substrate.[19] In this model, the stress generated at the interface is expressed also by Eq. (3) but with

$$\varepsilon_{\text{total}}=\varepsilon_{\text{substrate}}-\varepsilon_{\text{GaN}}=(\alpha_{\text{substrate}}-\alpha_{\text{GaN}})\times\Delta T, \qquad (5)$$

where α stands for the CTE and ΔT stands for the extent of temperature decrease from the film-formation temperature. The calculation results are illustrated in Fig. 5(b) for GaN growth on ZrB_2, SiC, and sapphire substrates at the film-formation temperature of 1073 K. The result for GaN growth on ZrB_2 at the film-formation temperature of 873 K is also shown in the figure for comparison. The film stress is zero at the film-formation temperatures, as assumed and it increases with decreasing temperature for all the substrates. The stress generated on cooling is in compression for ZrB_2 and sapphire substrates while it is in tension for the SiC substrate. The existence of the tensile stress in GaN films grown on 6H–SiC is consistent with the experimental observation.[20] This may indicates that the actual situation for GaN growth on top of 6H–SiC is close to this second model where misfit dislocations are introduced at the interface on the film formation so as to reduce the interfacial stress on the formation. For the sapphire substrate, the film stress at room temperature is the largest (266 MPa) even when the film stress on the formation at 1073 K is set to zero. This is due to the fact that the value of the CTE for sapphire is considerably larger than that for GaN. Of the three substrates, the stress generated in the GaN film is the smallest for the ZrB_2 substrate. When the film-formation temperature is reduced, the film stress at room temperature further decreases, for example, from 162 MPa at 1073 K to 120 MPa at 873 K.

The actual value of the stress developed in the GaN thin film may be between those deduced from these two extreme models, depending on the extent of relaxation due to the introduction of misfit dislocations at the interface. Nevertheless, ZrB_2 seems to be a substrate better than 6H–SiC and sapphire for heteroepitaxial growth of GaN, since the stress generated in GaN thin films is in compression and small when calculated with either of the two models. This comes obviously from the fact that the lattice mismatch between GaN and ZrB_2 is very small and the value of CTE for ZrB_2 is only a little larger than that for GaN.

V. CONCLUSION

(1) The values of the CTE along the *a*- and *c*-axis directions averaged over the temperature range from 300 to 1073 K are 6.66×10^{-6} and 6.93×10^{-6} K^{-1}, respectively. The isotropic thermal expansion behavior is somewhat surprising when the hexagonal crystal structure of ZrB_2, in which pure Zr and pure B atomic planes stack alternatively along the *c*-axis, is considered. The *a*-axis CTE value for ZrB_2 is only a little larger than that for GaN and is much smaller than that for sapphire.

(2) All the five independent single-crystal elastic constants are determined in the temperature range from room temperature to 1373 K by the RPR method. The elastic constants of ZrB_2 are best characterized by the large value of the Young modulus (as high as 500 GPa) and the low values of the Poisson ratio, c_{12} and c_{13}, indicating the stiffness and hardness and the brittleness, respectively. The orientation dependence of the Young modulus as well as the large c_{13}/c_{12} and small c_{33}/c_{11} values indicates that atomic bonding is stronger along the *a*-axis than along the *c*-axis, which is con-

sistent with the layered-type crystal structure stacked along the *c*-axis.

(3) The stresses developed in the GaN thin film grown on ZrB_2, 6H–SiC, and sapphire substrates are calculated with the use of the values of coefficient for thermal expansion and elastic constants of ZrB_2 determined in the present study. Of the three substrates, ZrB_2 is found to be the best for heteroepitaxial growth of GaN because of the smallest compressive stress developed in the GaN thin film.

ACKNOWLEDGMENTS

This work was supported by a Grant-in-Aid for Scientific Research (B) (12450282) from the Ministry of Education, Science, Sports, and Culture, Japan. The authors would like to thank Mr. Kawamoto, Shimazdu Co. Ltd., for the measurement of the coefficient of thermal expansion.

[1] *Interstitial Alloys*, edited by H. J. Goldschmidt (Butterworths, London, 1967).
[2] *Boron and Refractory Borides*, edited by V. I. Matkovich (Springer-Verlag, Berlin, 1977).
[3] *Progress in Boron Chemistry*, edited by R. J. Brotherton and H. Steinberg (Pergamon, New York, 1970), Vol. 2.
[4] A. S. Brown, Aerosp. Am. **35**, 20 (1997).
[5] H. Kinoshita, S. Otani, S. Kamiyama, H. Amano, I. Akasaki, J. Suda, and H. Matsunami, Jpn. J. Appl. Phys., Part 1 **40**, L1280 (2001).
[6] J. Suda and H. Matsunami, J. Cryst. Growth **237–239**, 1114 (2002).
[7] W. C. Hughes, W. H. Rowland, M. A. L. Johnson, S. Fujita, J. W. Cook, J. F. Schetzina, J. Ren, and J. A. Edmond, J. Vac. Sci. Technol. B **13**, 1571 (1995).
[8] Y. U. Melnik, I. P. Nikitana, A. S. Zubrilov, A. A. Sitnikova, Y. G. Musikhin, and V. A. Dimitriev, Inst. Phys. Conf. Ser. **142**, 863 (1996).
[9] T. Detchprohm, K. Hiramatsu, K. Itoh, and I. Akasaki, Jpn. J. Appl. Phys., Part 1 **31**, L1454 (1992).
[10] Y. Kato, S. Kitamura, K. Hiramatsu, and N. Sawaki, J. Cryst. Growth **144**, 133 (1994).
[11] X. H. Wu, P. Fini, S. Keller, E. J. Tarsa, B. Heying, U. K. Mishra, S. P. Den Baars, and J. S. Speck, Jpn. J. Appl. Phys., Part 1 **35**, L1648 (1996).
[12] R. A. Cutler, *Engineered Materials Handbook* (The Materials Information Society, Warrendale, PA, 1990), Vol. 4, p. 787.
[13] S. Otani and Y. Ishizawa, J. Cryst. Growth **165**, 319 (1996).
[14] S. Otani, M. M. Korsukova, and T. Mitsuhashi, J. Cryst. Growth **186**, 582 (1998).
[15] K. Tanaka and M. Koiwa, High Temp. Mater. Process. **18**, 323 (1999).
[16] H. P. Maruska and J. J. Tietjen, Appl. Phys. Lett. **15**, 327 (1969).
[17] F. A. Ponce, B. S. Krusor, J. S. Major, W. E. Plano, and E. F. Welch, Appl. Phys. Lett. **67**, 410 (1995).
[18] S. Nakamura, T. Mukai, and M. Senoh, J. Appl. Phys. **76**, 8189 (1994).
[19] X. H. Wu, L. M. Brown, D. Kapolnek, S. Keller, B. Keller, S. P. Den Baars, and J. S. Speck, J. Appl. Phys. **80**, 3228 (1996).
[20] T. Honda, N. Fujita, K. Maki, Y. Yamamoto, and H. Kawanashi, Appl. Surf. Sci. **159–160**, 468 (2000).
[21] R. R. Reeber and K. Wang, MRS Internet J. Nitride Semicond. Res. **6**, 3 (2001).